ChemComm

Accepted Manuscript

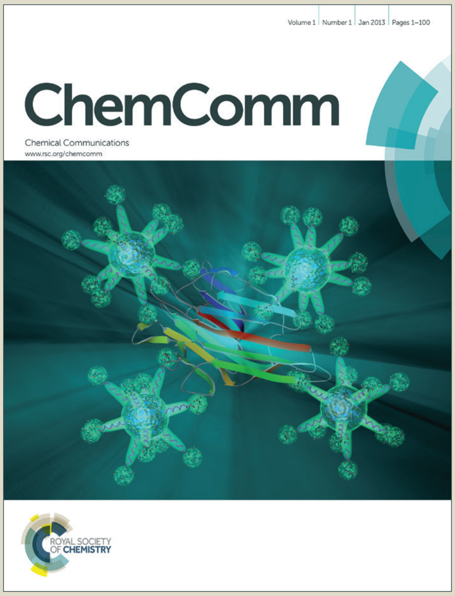

ROYAL SOCIETY OF CHEMISTRY

www.rsc.org/chemcomm

Journal Name

RSCPublishing

COMMUNICATION

In-Situ encapsulation of Pd inside the MCM-41 channel

aCite this: DOI: 10.1039/x0xx00000x

Xi-Jie Lin,[a,b] Ai-Zhi Zhong,[a,b], Yong-Bin Sun,[b] Xin Zhang,[b] Wei-Guo Song,[b] Rong-Wen Lu,*[a] An-Min Cao,*[b] Li-Jun Wan*[b]

Received 00th January 2012,
Accepted 00th January 2012

DOI: 10.1039/x0xx00000x

www.rsc.org/

Pd nanoparticles were successfully introduced into the channels of mesoporous silica MCM-41 with their dispersion well-tuned. We identified the dual functions played by CTAB, which was critical for both micelle template and Pd grafting, leading to the formation of a highly active Pd/MCM-41 nanocomposite for catalysing the Suzuki reaction.

Mesoporous silica has aroused great interest due to their interesting properties including uniform mesostructure, high surface area, and tunable pore size[1], which promised great potential in a large variety of areas such as adsorption[2], drug delivery[3], and catalysis[4]. Great efforts have been exerted on the synthesis of mesoporous silica, for example MCM-41, so that the size, shape and mesostructure can be tailored for improved performance. Equally important, the unique channel structure leaved huge room for their further functionalization since it can act as an ideal host for other materials. Typically, different metal nanoparticles can be loaded into the mesopore voids and form a metal/SiO_2 nanocomposite, which has been widely exploited as a model catalyst for different reactions.[5]

The synthetic protocols to introduce metal nanoparticles into the mesopores of silica can be briefly categorized into two groups. The first is usually known as a two-step procedure, which necessitates a post treatment step. After the preparation of the pristine silica, different techniques would be enforced such as impregnation[6], chemical vapour deposition[7], and sonochemical preparation[8]. The second group is known as the one-pot synthesis through a direct incorporation, which can effectively load the metals during the formation of the mesopores. For example, as reported by wang et al., a mercapto-containing agent was used to coordinate with Au cations. The strong interaction between these two will help to anchor Au into the channels during the formation of mesoporous silica.[9] Despite of the success in metal grafting through the above-mentioned methods, the current techniques were also known to have different disadvantages such as uncontrolled growth, unevenly distribution, low loading amount or complicated synthesis process. It is highly favourable that simple and easy ways could be developed so that metal nanoparticles can be effectively controlled so as to facilitate their further applications.

As for the metals, we have special interest in Pd, which is known as one of the most active catalysts for a large number of reactions such as hydrogenation[10], aerobic oxidation of alcohols[11], Heck reaction[12], and Suzuki cross coupling reaction[13]. Meanwhile, the active Pd nanoparticles can also be highly unstable. They will be subject to aggregate or leach during the reaction, resulting bad cyclability. Therefore it has been a common practice that Pd nanoparticles were immobilized by different supports, typically mesoporous silica.[14] From the point of view of a better catalyst design, the active Pd nanoparticles should be largely anchored inside the channels instead of sitting on the outer surface of the silica. Meanwhile, a good dispersion of the metals should be guaranteed without serious aggregation. In this way, different important parameters such as the size and the loading density of the nanocomposite can be well controlled, which has been a centre of interest in catalyst for decades.[15]

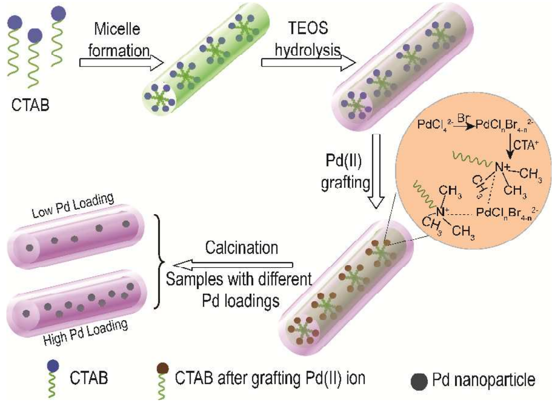

Scheme. 1 Scheme to show our one-pot synthesis route for Pd/MCM-41. CTAB played a double role as both the micelle template and the Pd grafting agent.

Herein we report a convenient method to encapsulate Pd nanoparticles inside the MCM-41 channels. Different from the conventional strategies, in which the surfactants for micelles were only used for the formation of mesoporous SiO_2, we identified that the surfactant of CTAB was very effective for grafting Pd species.

With its help, highly-dispersed and well-controlled Pd nanoparticles could be immobilized inside the channel of mesoporous SiO_2 through a one-pot reaction. Accordingly, these Pd nanoparticles were well protected by the channels, showing a high catalytic activity and notable cyclability for a typical Suzuki reaction.

We started with a typical synthesis for MCM-41 by using CTAB as the surfactant and tetraethoxysilane (TEOS) as the silica source (See supporting information for details). After 30 minutes reaction, these MCM-41 particles formed and the solution turned milky white. Instead of centrifuging the newly-formed m-SiO_2 out, we directly added in different amounts of $(NH_4)_2PdCl_4$ solution for Pd loading. Finally, the product was collected by means of the centrifugation-washing cycles and then a heat treatment in an H_2/Ar flow at 450 ^oC led to the formation of Pd/MCM-41. A detailed synthesis route could be found in Scheme 1.

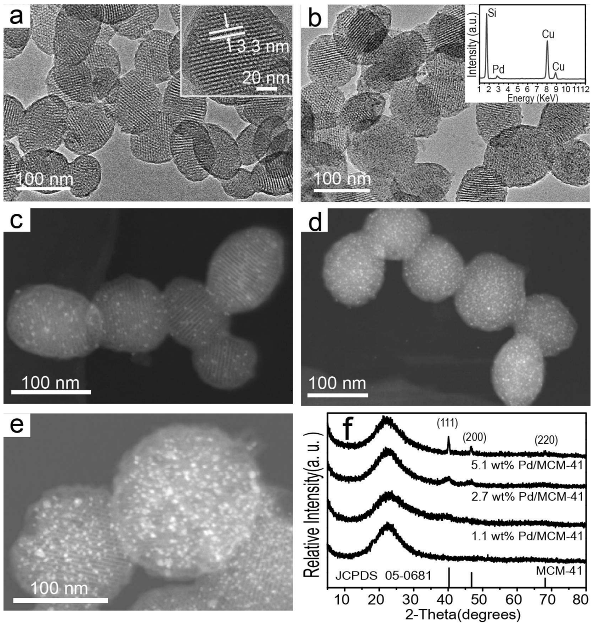

Fig. 1 (a-b) TEM images of MCM-41 (a) and 1.1 wt% Pd/MCM-41 (b) under a bright field operation mode; (c-e) STEM images for a series of Pd/MCM-41 nanocomposites with different Pd loadings: c) 1.1 wt%, d) 2.7 wt%, and e) 5.1 wt%, respectively. (f) XRD patterns for MCM-41 and the Pd/MCM-41 nanocomposites.

Fig. 1a showed a typical transmission electron microscopy (TEM) image of the MCM-41 particles after the hydrolysis of TEOS. The particles showed a diameter around 100 nm with characteristic mesoporous channels, whose pore size was around 3 nm as identified by the high resolution TEM image (HRTEM, inset in Fig. 1a). We found that the Pd grafting did not cause a drastic change on the particle shape of MCM-41. The particle size as well as its regular channels remained almost the same as revealed by the TEM image of the Pd/MCM-41 sample (Fig. 1b). However, different from the empty channels for blank MCM-41, tiny nanoparticles became discernible in the pores after the introduction of Pd (Fig. 1b), whose existence in the nanocomposite could be confirmed by the energy dispersion spectroscopy (EDS) shown in the inset. The inductively-coupled plasma atomic emission spectrometry (ICP-AES) showed that the Pd loading is around 1.1 wt%. A thorough TEM investigation revealed that most of the Pd nanoparticles sit well inside the channels although independent Pd particles on the surface of MCM-41could also be found sporadically. It turned out that our synthesis route was very effective in grafting the Pd species inside the channels of MCM-41 with no notable escape.

Due to the low phase contrast between the silica matrix and the incorporated Pd, it was not very easy to have a clear TEM image of the Pd nanoparticles under the normal bright-field TEM mode. Therefore, we resorted to the scanning TEM (STEM) characterization under a dark filed mode so as to have a better differentiation. Fig. 1c showed the corresponding STEM image of the same sample showed in Fig. 1b. The Pd nanoparticles became much easier to be observed from their silica background. It was obvious that these Pd were independent from each other and they were well dispersed inside the channels. Due to the pore confinement, these Pd showed a small size around 3 nm with no further growth. We found that it was very convenient to control the dispersion of Pd nanoparticles by varying the Pd loadings. As for nanocomposite with an increased Pd amount of 2.7 wt%, more Pd nanoparticles formed inside the channels as revealed those white dots shown in Fig. 1d. This trend became more obvious for the sample with 5.1 wt% Pd (Fig. 1e). Similarly, almost all the Pd nanoparticles were encaved inside the pores and no independent Pd nanoparticles could be observed aside from the MCM-41, confirming the effectiveness of Pd grafting in our synthesis. The XRD patterns for the Pd-containing samples were shown in Fig. 1f. The weak but distinguishable peaks showed a characteristic pattern for crystalline Pd (JCPDS 05-0681) as the weight loadings of Pd increased.

A direct benefit from this encapsulation was the obviously-improved thermal stability of Pd nanoparticles inside the MCM-41 channels. Usually, high temperature treatment would result in the deformation and aggregation of nanoparticles, leading to a sintering of small particles.[16] In benefit of the channels, the inside Pd nanoparticles was able to sustain a high temperature treatment up to 800 ^oC. As shown in Fig. 2a, the Pd particles were confined well inside the channels and remained a tiny particle size with no big increase. Finally at 900 ^oC we started to see big chunks of Pd particles with a diameter around 20 nm due to the sintering (Fig. S1). For comparison, a sample with Pd nanoparticles supported on the surface of SiO_2 (Fig. S2), instead of inside the SiO_2 mesopores, was also prepared (see supporting information for synthesis details). It turned out that these tiny Pd nanoparticles would sinter even at 600 ^oC as shown in Fig. 2b.

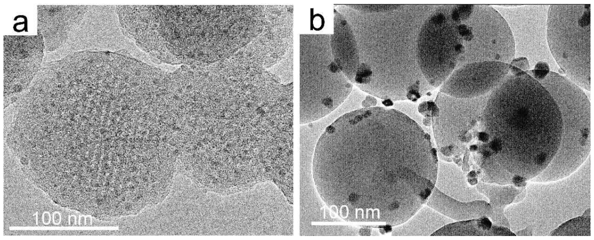

Fig. 2 TEM images of: (a) Pd/MCM-41 after heat treatment at 800 ^oC. Regular channel structure could be remained and Pd nanoparticles dispersed well without aggregation due to the existence of channel; (b) Pd-SiO_2 which the Pd nanoparticles supported on the SiO_2 surface sintered seriously after heating at 600 ^oC.

The N_2 absorption/desorption isotherms which presented in Fig. S3 exhibited that this materials has relatively high specific surface area. Calculated by the Brunauer-Emmett-Teller (BET) method, the specific surface areas of MCM-41 and Pd/MCM-

41 were found to be 935 m^2/g and 984 m^2/g, respectively. It can be found that the specific surface area only changed a little after introducing Pd. This phenomenon demonstrated that the introduction of Pd did not affect the mesoporous structure of the material, which conformed to the STEM images provided above. Meanwhile, the pore size distribution curves of these two samples were also similar as shown in figure S4. It was interesting that the pore size of Pd/MCM-41 increased a little from 3.0 nm to 3.3 nm. It turned out that the introduction of Pd species inside the micelles did affect their structure to some extent, finally resulting in a slightly larger pore size. Despite of such a tiny difference, it was obviously that the Pd/MCM-41 was mesoporous with characteristic channels. The incorporation of Pd nanoparticles into channels would not destroy their mesopores, and Pd nanoparticles could be well confined in the channels so that serious aggregation would be avoided.

We found that the existence of CTAB was critical for a successful grafting of Pd inside the mesopores. A blank MCM-41 sample with CTAB removed failed to graft Pd as confirmed in a control experiment. Specifically, the MCM-41 sample was collected and then subjected to a heat treatment at 550 °C in air so that CTAB could be totally removed. This MCM-41 sample was then dispersed in solution and $(NH_4)_2PdCl_4$ was introduced. The suspension showed a brown colour as contrasted to the milk white one which was successful for Pd grafting (Fig. S5). The TEM images (Fig. S6) also confirmed that the Pd particles did not be encapsulated inside the channel but existed outside the pores with serious aggregation. The UV-vis spectrum revealed that there existed interaction between $(NH_4)_2PdCl_4$ and CTAB. As shown in Fig. S7, the mixed solution of CTAB and $(NH_4)_2PdCl_4$ exhibited two new bands near 250 nm and 340 nm, which could not be observed from neither of them. The interaction between CTAB and Pd(II) has been discussed by different groups[17] and the formation of $[CTA]_2[PdCl_nBr_{4-n}]$ (n=0~4) was suggested during the preparation of Pd nanoparticles. Here speculated that this ligand exchange also happened in our synthesis as revealed by the new peaks in the UV-vis spectra and the indispensable role played by CTAB. By means of this palladate-CTAB interaction, it turned possible that the Pd species could be successfully grafted into the channels of the MCM-41 with CTAB sitting inside.

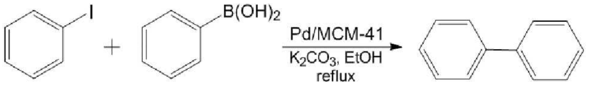

Scheme. 2 Suzuki cross-coupling reaction of iodobenzene with phenyl boronic acid.

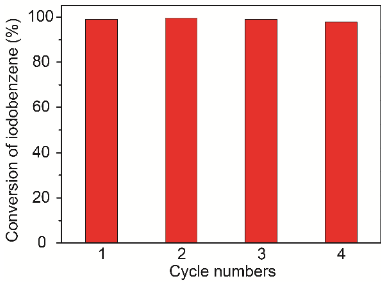

Fig. 3 Cyclability tests of the Pd/MCM-41 catalyst. The conversion of iodobenzene was measured after 15 minutes' reaction.

Inspired by the mesoporous structure of MCM-41 and the highly dispersed Pd nanoparticles inside the channels, we expected that this Pd/MCM-41 nanocomposite could be an effective and stable catalyst for Suzuki cross coupling reaction. Here we used the reaction between iodobenzene and phenylboronic acid as a test experiment to investigate the catalytic properties of the as-prepared Pd/MCM-41. Scheme 2 showed the reaction route between iodobenzene and phenylboronic acid for biphenyl assisted by the 1.1 wt% Pd/MCM-41 nanocomposite. In this reaction, we measured the catalytic activity by using the turnover frequency (TOF) which represented the turnover number of iodobenzene per unit time. Interestingly, the nanocomposite showed a very promising catalytic activity with a 91.42% conversion of iodobenzene in just 5 minutes, and a TOF value of 98.25 min^{-1}.[18] Meanwhile, this Pd/MCM-41 nanocomposite showed a good cyclability and we didn't observe an obvious decay in catalytic activity upon extended runs. A demonstrative experiment showed that this Pd/MCM-41catalyst maintained a high conversion of iodobenzene about 96.63% after 4 continuous runs. The TEM image (Fig. S8) of the sample after the reaction cycles showed no obvious aggregation of Pd nanoparticles. Similarly, the ICP-AES test did not find the existence of Pd species inside the solution after the Suzuki reaction. The successful prevention of Pd leaching further confirmed the high stability of these nanoparticles due to the protection of the rigid channels[19]. These results demonstrated that this Pd/MCM-41 nanocomposite material obtained by our method has outstanding catalytic activity and cyclability, which are promising characters for their practical applications.

Conclusions

In summary, we developed a simple and effective method for the controlled anchoring of Pd nanoparticles inside the channels of MCM-41. The micelle template of CTAB was found to be critical for the grafting of Pd precursor, probably thorough the palladate-CTAB interaction. In this way, Pd nanoparticles could form inside the pores of MCM-41 with good dispersion. Due to the confinement of MCM-41 channels, the Pd nanoparticles were well protected and showed extraordinary thermal stability. We also identified that the Pd/MCM-41 nanocomposite could be a promising catalyst for Suzuki reaction as revealed by its prominent catalytic activity and cyclability.

Acknowledgement

This work was supported by the National Natural Science Foundation of China (Grants No. 21176038), the major State Basic Research Program of China (973 program: 2013CB934000, 863 program: 2013AA030800).

Notes and references

[a] State Key Laboratory of Fine Chemicals, Dalian University of Technology, Dalian, 116024, P. R. China.

[b] Key Laboratory of Molecular Nanostructure and Nanotechnology and Beijing National Laboratory for Molecular Sciences, Institute of Chemistry, Chinese Academy of Sciences (CAS), Beijing 100190, P. R. China.

E-mail: lurw@dlut.edu.cn, anmin_cao@iccas.ac.cn, wanlijun@iccas.ac.cn

† Electronic Supplementary Information (ESI) available: Experimental details, characterization, and data. See DOI: 10.1039/b000000x/

1 J. Y. Ying, C. P. Mehnert and M. S. Wong, *Angew. Chem. Int. Ed.*, 1999, **38**, 56-77.

2 A. Vinu, V. Murugesan and M. Hartmann, *J. Phys. Chem. B.*, 2004, **108**, 7323-7330.

3 M. Vallet-Regi, F. Balas and D. Arcos, *Angew. Chem. Int. Ed.*, 2007, **46**, 7548-7558.

4 A. Taguchi and F. Schuth, *Micropor. Mesopor. Mat.*, 2005, **77**, 1-45.

5 S. H. Wu, C. Y. Mou and H. P. Lin, *Chem. Soc. Rev.*, 2013, **42**, 3862-3875.

6 Z. J. Wang, Y. B. Xie and C. J. Liu, *J. Phys. Chem. C.*, 2008, **112**, 19818-19824.

7 S. Suvanto, J. Hukkamaki, T. T. Pakkanen and T. A. Pakkanen, *Langmuir*, 2000, **16**, 4109-4115.

8 S. Zhu, D. Zhang, X. Zhang, L. Zhang, X. Ma, Y. Zhang and M. Cai, *Micropor. Mesopor. Mat.*, 2009, **126**, 20-25.

9 S. Wang, Q. Zhao, H. Wei, J.-Q. Wang, M. Cho, H. S. Cho, O. Terasaki and Y. Wan, *J. Am. Chem. Soc.*, 2013, **135**, 11849-11860.

10 Z. H. Guan, S. M. Lu and C. Li, *J. Catal.*, 2014, **311**, 1-5.

11 C. Liu, J. Wang, L. K. Meng, Y. Deng, Y. Li and A. W. Lei, *Angew. Chem. Int. Ed.*, 2011, **50**, 5144-5148.

12 Y. Wan, H. Y. Wang, Q. F. Zhao, M. Klingstedt, O. Terasaki and D. Y. Zhao, *J. Am. Chem. Soc.*, 2009, **131**, 4541-4550.

13 B. Z. Yuan, Y. Y. Pan, Y. W. Li, B. L. Yin and H. F. Jiang, *Angew. Chem. Int. Ed.*, 2010, **49**, 4054-4058.

14 C. M. Crudden, M. Sateesh and R. Lewis, *J. Am. Chem. Soc.*, 2005, **127**, 10045-10050.

15 S. Jana, B. Dutta, R. Bera and S. Koner, *Inorg. Chem.*, 2008, **47**, 5512-5520.

16 S. H. Joo, J. Y. Park, C.-K. Tsung, Y. Yamada, P. Yang and G. A. Somorjai, *Nat. Mater.*, 2009, **8**, 126-131.

17 B. Veisz and Z. Kiraly, *Langmuir*, 2003, **19**, 4817-4824.

18 S. Jana, S. Haidar and S. Koner, *Tetrahedron Lett.*, 2009, **50**, 4820-4823.

19 S. Y. Ding, J. Gao, Q. Wang, Y. Zhang, W. G. Song, C. Y. Su and W. Wang, *J. Am. Chem. Soc.*, 2011, **133**, 19816-19822.